

MICROLENSING OF BLENDED STELLAR IMAGES

Przemysław Woźniak and Bohdan Paczyński

Princeton University Observatory, Princeton, NJ 08544–1001, USA

e-mail: wozniak@astro.princeton.edu, bp@astro.princeton.edu

ABSTRACT

The current modelling of single microlensing light curves neglects the possibility that only a fraction of the light is due to the lensed star, the remaining being due to a close, unresolved blend, which may be related or unrelated to the lens.

Unfortunately, the effects of blending are significant as all microlensing experiments choose very crowded fields as their targets. In this paper we point out a strong degeneracy of the fitting procedure which makes it practically impossible to detect the presence of a blend by purely photometric means, except in a small part of the parameter space. Some blends may be detected by astrometric means, but the majority have to be corrected for statistically. The luminosity function reaching well below the ground based detection limit (with the HST) would be very helpful. The statistics of binary stars in the target population is also important and this could be determined with the repeating microlensing events.

If no correction is made then the event time scales, the lens masses, and the optical depth are all systematically underestimated.

Subject headings: galaxy: structure – ISM: extinction – photometry

1. Introduction

Almost all model fitting of single microlensing light curves to the data is done with a 4-parameter curve which assumes that the stellar image is not blended (cf. Paczyński 1996, and references therein). However, the first two double lenses: OGLE #7 (Udalski et al. 1994b) and DUO #2 (Alard et al. 1995) were found to have apparent images made of at least two objects: the lensed star and another unrelated star. Also, at least one single event, OGLE #5, was found to be strongly blended (Mao 1995, Alard 1996b). According to Alard (1996b) most DUO events are likely to be blended, and fitting data with unblended

light curves introduces a systematic bias in the estimate of event time scales and optical depth. Other effects of blending were considered by Nemiroff (1994), Di Stefano & Mao (1995), and by Buchalter & Kamionkowski (1996).

Another issue is the lensing of very faint stars which become detectable only while lensed (Nemiroff 1994). Such objects are missed in searches like DUO (Alard 1996a), EROS (Auburg et al. 1993), MACHO (Alcock et al. 1993) and OGLE (Udalski et al. 1993), but they are detectable in the searches which use the “image subtraction” technique, like AGAPE (Bouquet et al. 1996) and COLUMBIA–VATT (Crotts & Tomaney 1996, Tomaney & Crotts 1996, 1997). An elaborate theory of this technique was developed by Gould (1996).

The aim of this paper is to demonstrate some of the practical consequences of blending, and the limitations imposed by unknown blends on the determination of lens parameters.

2. The Model

Let us consider an idealized situation with a variability due to microlensing superposed on arbitrary constant background of whatever nature: the sky, or the crowded field made of many stars or nebulae. We adopt an approximation according to which in a given small aperture (it may be profiled as the PSF, the Point Spread Function) there is a well measured level of brightness long before and long after the microlensing event:

$$F_0 \pm \Delta_0 N_0^{-1/2}, \quad N_0 \gg 1, \quad (1)$$

where Δ_0 refers to a standard deviation of a single measurement, and the number of measurements N_0 is very large. Therefore, F_0 as well as Δ_0 are known very accurately. However, we do not know what fraction of F_0 is due to the star which is microlensed while it is in its normal, unlensed condition.

Let the flux from the lensed star be given as

$$F_s = F_{s0} A(t), \quad F_{s0} = f_s F_0 < F_0, \quad (2)$$

where the magnification due to microlensing is

$$A(t) = \frac{u^2 + 2}{u (u^2 + 4)^{1/2}}, \quad u^2(t) = u_{min}^2 + \left(\frac{t - t_{max}}{t_0} \right)^2, \quad (3)$$

where u_{min} is the impact parameter in units of Einstein ring radius, t_{max} is the time at which maximum magnification is reached, and t_0 is the time it takes the lens to move with respect to the source by one Einstein ring radius (Paczynski 1996, and references therein).

Given a set of photometric measurements: (F_k, t_k) , $i = 1, 2, 3, \dots, n$, we would like to determine four parameters: F_{s0} , u_{min} , t_{max} , t_0 . In principle the value of the fifth parameter: F_0 has to be determined as well. However, in practice a good microlensing search is conducted over a time interval much longer than the microlensing time scale t_0 , so we may simplify our task by adopting F_0 as known. In a common fitting procedure it is assumed that $F_{s0} = F_0$, and F_0 has to be determined from the same set of measurements as the other three parameters: u_{min} , t_{max} , t_0 .

We assume that the errors (standard deviations) of the measurements scale as

$$\Delta_k = \left(\frac{F_k}{F_0}\right)^{1/2} \Delta_0, \quad \left(\frac{F_k}{F_0}\right) = (1 - f_s) + f_s A(t_k), \quad f_s \equiv \frac{F_{s0}}{F_0}, \quad (4)$$

where Δ_0 is the error of a single measurement at intensity F_0 , f_0 is the fractional intensity of the lensed star far from the microlensing event, and the magnification $A(t_k)$ is given with the eq. (3). Our task is to find out how accurately the lens parameters can be determined. Instead of a massive Monte–Carlo simulation we adopt another approach. First, the values of F_0 , Δ_0 , f_s , u_{min} , t_{max} , t_0 are fixed. The first two are assumed to be known to the observer, while the latter four are to be determined. The χ^2 of the fit between a model and a string of quasi-data points $(F_{data,k}, t_k)$, $k = 1, 2, 3, \dots, n$ is approximated with the sum:

$$X^2 = \sum_{k=1}^n \frac{(F_{model,k} - F_{data,k})^2 + \Delta_k^2}{\Delta_k^2}, \quad (5a)$$

$$F_{model,k} = (F_0 - F_{s0}) + F_{s,k}, \quad (5b)$$

where $F_{model,k}$ are the intensities which follow from the model we are fitting, the quasi-observations $F_{data,k}$ are given with the eq. (2), and the measurement errors Δ_k are given with the eq. (4). Our task is to determine the values of four parameters: $\alpha_{1,2,3,4} = (f_s, u_{min}, t_{max}, t_0)$ by minimizing X^2 . Note that because of measurement errors the value of X^2 can never be zero. It is minimized for the correct choice of the four parameters, when its value is n . We shall also determine the confidence ranges of the four parameters for which the value of X^2 is within a chosen range of its minimum. For simplicity we assume that n equally spaced measurements cover the time interval $t_{max} - 2t_0 < t < t_{max} + 2t_0$.

For small errors we can expand X^2 around its minimum to obtain:

$$\Delta X^2 \simeq \sum_{j=1}^4 \sum_{i=1}^4 D_{i,j} \Delta \alpha_i \Delta \alpha_j, \quad (6)$$

where $\Delta\alpha_i = \alpha_{model,i} - \alpha_{data,i}$ ($i = 1, 2, 3, 4$) is a vector of the parameter differences between the fitting and the model values, and

$$D_{ij} = \frac{F_0}{\Delta_0^2} \sum_{k=1}^n \frac{1}{F_k} \left[\frac{\partial F_k}{\partial \alpha_i} \frac{\partial F_k}{\partial \alpha_j} \right], \quad (7)$$

at $\alpha_i = \alpha_{data,i}$, ($i = 1, 2, 3, 4$). For a quadratic expansion the confidence ellipsoid it describes scales linearly with the measurement errors. The errors with which all model parameters are determined scale linearly with the quantity $a \equiv \Delta_0 n^{-1/2}$, for $n \gg 1$ and $\Delta_0 \ll 1$.

The best MACHO and OGLE microlensing events had $n \approx 60$ and $\Delta_0 \approx 0.04$, for the corresponding $a \approx 0.005$ (cf. Udalski et al. 1994a, Alcock et al. 1995). A more typical values were $(n, \Delta_0, a) \approx (30, 0.1, 0.02)$. However, with the introduction of effective follow-up observations by the PLANET (Albrow et al. 1996) and GMAN (Pratt et al. 1996). a substantial increase of n , a reduction of Δ_0 , and the corresponding reduction of the parameter a have already been achieved in some cases, and farther improvement is expected in the near future.

In the following section we investigate some problems with the determination of model parameters imposed by the finite value of the a parameter.

3. The Degeneracy

There are two regions in the parameter space for which there is a near degeneracy, i.e. with any realistic accuracy of the measurements it is not possible to determine the unique values of all model parameters.

The first troublesome case is that of a large impact parameter. In the limit $u_{min} \gg 1$ the eqs. (2) and (3) may be transformed as follows:

$$A \approx 1 + \frac{2}{u^4} = 1 + \frac{2}{[u_{min}^2 + (t/t_0)^2]^2}, \quad \text{for } u \gg 1, \quad t_{max} = 0. \quad (8)$$

Within this approximation we can write (cf. eqs. 2-4)

$$\frac{F(t)}{F_0} = (1 - f_s) + f_s \times \left(1 + \frac{2}{[u_{min}^2 + (t/t_0)^2]^2} \right) = 1 + \frac{2f_s}{[u_{min}^2 + (t/t_0)^2]^2}. \quad (9)$$

It is straightforward to verify that substituting the parameters

$$f_{s,1} = f_s C^4, \quad u_{min,1} = u_{min} C, \quad t_{0,1} = t_0 C^{-1}, \quad (10)$$

into the eq. (9) we recover the same formula for the F_s/F_0 . Therefore, if the set of parameters: (f_s, u_{min}, t_0) is a solution then the set $(f_s C^4, u_{min} C, t_0 C^{-1})$ is also a solution, where C is an arbitrary positive constant which satisfies $f_s C^4 \leq 1$.

Analytical considerations seem to imply that the trouble sets in when the impact parameter is very large, $u_{min} \gg 1$. In reality the situation is much worse. An example of the problem is shown in Fig. 1a, in which the two light curves shown with a solid and a dashed line, respectively, are almost identical. The truly troublesome aspect of this example is the value of the impact parameter: $u_{min} = 0.5$. This implies that in practice the degeneracy covers a broad range of impact parameters, and a seemingly robust microlensing event with the peak magnification in excess of 2 may have a blend which is photometrically undetectable in the event’s light curve.

Another troublesome case is when the minimum flux, i.e. the flux measured far from the microlensing event, is dominated by a blend or by any background. This is a generic case in very crowded fields, like the bulge of M31, in which microlensing events are to be detected by the “image subtraction” method (Bouquet et al. 1996, Crots & Tomaney 1996, Tomaney & Crots 1996, 1997). As the lensed object contributes little to the total light at minimum, the microlensing event can be detected only when the peak magnification is very large, i.e. the impact parameter is very small. In this case we have $F_{s0}/F_0 \ll 1$, $A_{max} \gg 1$, $u_{min} \ll 1$, and a significant change in the brightness occurs only close to t_{max} when the projected distance between the source and the lens is very small, i.e. when $u \ll 1$. We have

$$A \approx 1 + \frac{1}{u} \gg 1, \quad \text{for } u \ll 1, \quad (11)$$

and therefore

$$\frac{F(t)}{F_0} = (1 - f_s) + f_s A \approx 1 + \frac{f_s}{u} = 1 + \frac{f_s}{[u_{min}^2 + (t/t_0)^2]^{1/2}}, \quad \text{for } f_s \ll 1, \quad t_{max} = 0. \quad (12)$$

It is straightforward to verify that substituting the parameters

$$f_{s,1} = f_s C, \quad u_{min,1} = u_{min} C, \quad t_{0,1} = t_0 C^{-1}, \quad (13)$$

into the eq. (12) we recover the same formula for the F_s/F_0 . Therefore, if the set of parameters: (f_s, u_{min}, t_0) is a solution then the set $(f_s C, u_{min} C, t_0 C^{-1})$ is also a solution, where C is an arbitrary positive constant which satisfies $f_s C \leq 1$. An example of such a case is shown in Fig. 1b.

A more quantitative way to analyze the degeneracy is to plot the confidence contours in the $t_0 - u_{min}$ and in the $f_s - u_{min}$ planes. Two sets of such plots are shown in Fig. 2; they correspond to the two cases presented in Fig. 1. It is apparent that the contours are

highly elongated, i.e. a certain combination of model parameters may be determined with a reasonable accuracy, while the other combination is subject to a very large error. The photometric accuracy parameter $a \equiv \Delta_0/\sqrt{n} = 0.007$ was assumed, which may be achieved for example when $\Delta_0 = 0.05$ and $n = 50$.

The time of maximum magnification, t_{max} , and the peak brightness, F_{max} are not subject to any degeneracy in their determination as long as there are many points within FWHM of the light curve. Unfortunately, these two parameters are of no particular significance for any inferences from the microlensing observations. Those parameters which are significant: the event time scale t_0 and the impact parameter u_{min} tend to have strongly correlated errors, as shown in Fig. 2. It is a general property of blended microlensing events that some combination of the (t_0, u_{min}) values can be determined with a good accuracy, while some other can be determined only poorly. In both cases of degeneracy as described with the eqs. (10) and (13) the product $t_0 \times u_{min}$ can be measured well, but the ratio t_0/u_{min} cannot be determined from the observations, as it can be equal to any number. Therefore, we cannot determine the values of t_0 and u_{min} in these cases, only the value of the product of the two parameters. Note, that in accordance with this analytical reasoning the confidence contours as shown in the $t_0 - u_{min}$ plane in Fig. 2 appear to be stretched along a hyperbolic shape.

There are two dimensionless parameters which determine the shape of a blended microlensing light curve: the impact parameter u_{min} , and the fraction of minimum light contributed by the lensed source, $f_s \equiv F_{s0}/F_0$. For a chosen value of the accuracy parameter $a = 0.007$ we calculated values of the standard deviations in the determination of all four parameters: F_{s0} , u_{min} , t_0 , t_{max} as a function of F_{s0}/F_0 and u_{min} , and they are presented in Fig. 3. The lines are labeled with the values of standard deviation. For example, in the upper left corner the error in the determination of the fraction of light in the lensed object, $\delta F_{s0}/F_{s0}$ is equal 1.0 (i.e. a huge error) along the uppermost line, and the error is modest at 0.1 along the lowest line. If the accuracy parameter is smaller by a factor 10, i.e. if $a = 0.0007$, then the labels along all lines would be reduced by a factor 10, i.e. the accuracy of the determination of F_{s0}/F_0 would be 0.1 along the uppermost line, and 0.01 along the lowest line. A reduction of the a parameter by a factor 10 can be accomplished by reducing the photometric error Δ_0 by a factor 10, or by increasing the number of photometric measurements n by a factor 100.

An inspection of the Fig. 3 reveals that only the time of maximum magnification t_{max} can be well determined over a significant fraction of the parameter space. The other three parameters: F_{s0} , u_{min} , t_0 are virtually impossible to measure above the lines with the label 1.0. Note that our choice of the accuracy parameter a was optimistic by the standards of

current microlensing seraches.

As the confidence contours are so elongated (cf. Fig. 2) it is interesting to check if the best combination of the interesting parameters can be measured with a significantly higher accuracy than possible for each of the parameters separately. This is shown in Fig. 4, where the right two panels present the lines labelled with the corresponding values of a standard deviation for the best linear combination of $(u_{min}, F_{s0}/F_0)$ (upper right panel) and (u_{min}, t_0) (lower right panel). Note, lines in these panels are placed much higher than the corresponding lines in Fig. 3, i.e. the errors are strongly reduced by choosing the best combination of the parameter pairs, corresponding to the short axis of the elliptical confidence contours in Fig. 2. On the other hand, the opposite choice, corresponding to the long axis of the elliptical confidence contour, and presented in the two left hand panels in Fig. 4, reveal errors even larger than those corresponding to each parameter separately, as presented in Fig. 3.

Let us now ignore the presence of blends, and let us follow the standard procedure, assuming that $F_{s0} = F_0$. With this assumption we determine the values of the event time scale t'_0 and the impact parameter u'_{min} . The parameters so determined may be compared with their true values t_0 and u_{min} in Fig. 5. It is clear that by neglecting the blend we always overestimate u_{min} and we underestimate t_0 , with the error increasing towards lower values of F_{s0}/F_0 , i.e. stronger blending, and lower values of impact parameter.

With the blending effects being so important we should check when the presence of the blend can be established by means of photometry alone. It was done so with the two double lenses (OGLE #7, Udalski et al. 1994b; DUO #2, Alard et al. 1995) and with one single lens (OGLE #5, S. Mao, private communication 1995, Alard 1996b). Unfortunately, this task is difficult for events caused by a single point mass, as shown in Fig. 6, where the change in the value of X^2 is shown as a function of two dimensionless parameters: F_{s0}/F_0 and u_{min} . This is the difference between the X^2 values of a blended event as fitted with and without a blend. If the change is large then photometry alone can clearly demonstrate that the lensed source has a blend. The parameter space above the thick line $\Delta X^2 = 2.8$ is photometrically degenerate: in this region it is not possible to detect the presence of a blend with the photometric accuracy parameter $a = 0.007$ at the confidence level 90%.

4. Discussion

The main result of this paper is somewhat discouraging: with the currently typical photometric coverage and accuracy the light curve of a single microlensing event cannot be

used to determine the presence of a blend unless the impact parameter is small, $u_{min} < 0.3$, and the blend may be photometrically undetectable even if the impact parameter is very small (cf. Fig. 6). In the real world we do not know the precise value of the measurement errors, and there is a significant contribution to the errors which is non-gaussian (Udalski et al. 1994a). Therefore, the photometric border of blend detectability as indicated by the thick line in Fig. 6 is optimistic, with the true border located at even lower values of u_{min} . Yet, the blending must be very common as demonstrated by the two double lensing events (OGLE #7, Udalski et al. 1994a; DUO #2, Alard et al. 1995), and by the recent analysis of the DUO results (Alard 1996b). Unless the blending is somehow corrected for, the microlensing time scales t_0 are underestimated, and the impact parameters are overestimated (cf. Fig. 5). This implies that the lens masses and the optical depth are systematically underestimated.

There are various ways in which the blending may be detected or at least statistically corrected for, as discussed by Alard (1996b). In case of a double lens, with caustic crossings indicated by the light curve, a blend reduces the apparent magnification between caustic crossings below the theoretical minimum value $A_{min} = 3$ (Witt & Mao 1995) – this was apparent in OGLE #7 and in DUO #2. In case of any event, double or single, a blend can be detected through a correlation between the image centroid and the apparent brightness, as first noticed in DUO #2 (Alard et al. 1995). This is possible if the angular separation between the lensed object and the blend is not too small, presumably no less than half a pixel, or so. If the blend has a different color than the lensed star then it may be uncovered with multi band lightcurves of a microlensing event (Buchalter & Kamionkowski 1996). If the luminosity function well below the detection threshold is known, say from the HST imaging, then the blending can be statistically corrected for by placing artificial stellar images on the CCD frames.

The last approach has its limitations. As long as we do not know the distribution of separations and luminosity ratios of binary stars in the target population we can only put artificial stars randomly on a CCD frame. But this procedure will underestimate the number of very close binary pairs. Fortunately, if the detected number of microlensing events is very large we can use the microlensing itself to determine the statistics of binary stars, as they will produce repeating microlensing events (Di Stefano & Mao 1996).

This work was supported with the NSF grants AST–9313620 and AST–9530478.

REFERENCES

- Alard, C. 1996a, in IAU Symp. 173: “Astrophysical Applications of Gravitational Lensing”, (Eds.: Kochanek, C. S., & Hewitt, J. N., Kluwer Academic Publishers), p. 215
- Alard, C. 1996b, A&A, in press (= astro-ph/9609165)
- Alard, C., Mao, S., & Guibert, J. 1995, A&A, 300, L17
- Albrow, M. et al. 1996, preprint: astro-ph/9610128, to appear in the Proceedings of the 12th IAP Conference (Eds. R. Ferlet and J.-P. Maillard): “Variable Stars and the Astrophysical Returns of Microlensing Surveys”
- Alcock, C. et al. 1993, Nature, 365, 621
- Alcock, C. et al. 1994, preprint: astro-ph/9512146
- Aubourg, E. et al. 1993, Nature, 365, 623
- Bouquet, A. et al. 1996, to appear in the Proceedings of the 12th IAP Conference (Eds. R. Ferlet and J.-P. Maillard): “Variable Stars and the Astrophysical Returns of Microlensing Surveys”
- Buchalter, A., & Kamionkowski, M. 1996, ApJ, 469, 676
- Crotts, A., & Tomaney, A. 1996, ApJ, 473, L87
- Di Stefano, R., & Mao, S. 1996, ApJ, 457, 93
- Gould, A. 1996, ApJ, 470, 201
- Nemiroff, R. J. 1994, ApJ, 435, 682
- Paczynski, B., 1996, ARA&A, 34, 419
- Pratt, M. R. et al. 1996, in IAU Symp. 173: “Astrophysical Applications of Gravitational Lensing”, (Eds.: Kochanek, C. S., & Hewitt, J. N., Kluwer Academic Publishers), p. 221 (= astro-ph/9508039)
- Udalski, A. et al. 1993, AcA, 43, 289
- Udalski, A. et al. 1994a, AcA, 44, 165
- Udalski, A. et al. 1994b, ApJ, 436, L103
- Tomaney, A., & Crotts, A. 1996, AJ, 112, 2872
- Tomaney, A., & Crotts, A. 1997, to appear in the Proceedings of the 12th IAP Conference (Eds. R. Ferlet and J.-P. Maillard): “Variable Stars and the Astrophysical Returns of Microlensing Surveys”

Witt, H. J., & Mao, S. 1995, ApJ, 447, L105

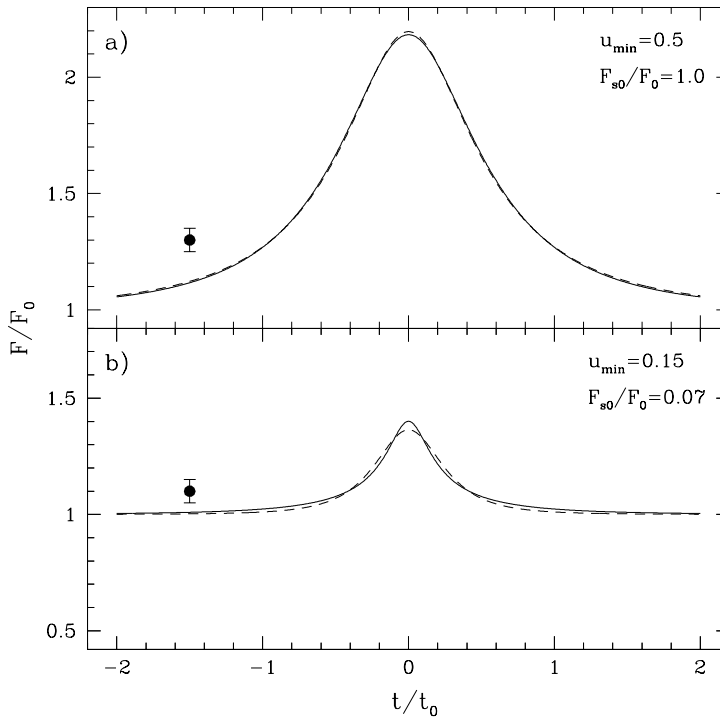


Fig. 1.— Two examples of degeneracy are shown. (a) A large impact parameter. The unblended event with $u_{min} = 0.5$ and $t_0 = 1.0$ (solid) is well fitted by the model with $u'_{min} = 0.4$, $t'_0 = 1.15$ and $F_{s0}/F_0 = 0.73$ (dashed). The difference in the goodness of fit as defined with eqs. (5) is $\Delta X^2 = 0.52$. (b) A strong blending. The solid line shows the microlensing light curve with the parameters: $u_{min} = 0.15$, $t_0 = 1.0$, $F_{s0}/F_0 = 0.07$. The dashed light curve is the best light curve for unblended event with $u'_{min} = 0.97$, $t'_0 = 0.30$. The difference between the two corresponds to $\Delta X^2 = 2.63$. In both plots a large dot with the error bar indicates Δ_0 , the photometric error at minimum light.

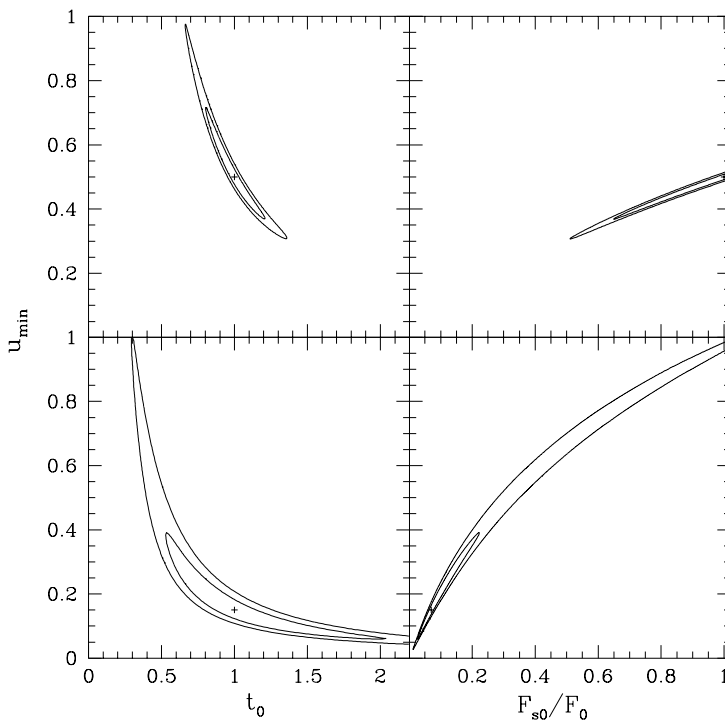


Fig. 2.— Confidence contours in the $(t_0 - u_{min})$ and $(F_{s0}/F_0 - u_{min})$ planes for two cases of degeneracy from Fig. 1: a large impact parameter ($u_{min} = 0.5$, upper) and a strong blending ($F_{s0}/F_0 = 0.07$, lower). Confidence levels are 68% and 90% for one parameter of interest. The photometric accuracy parameter $a = \Delta_0/\sqrt{n} = 0.007$ was adopted.

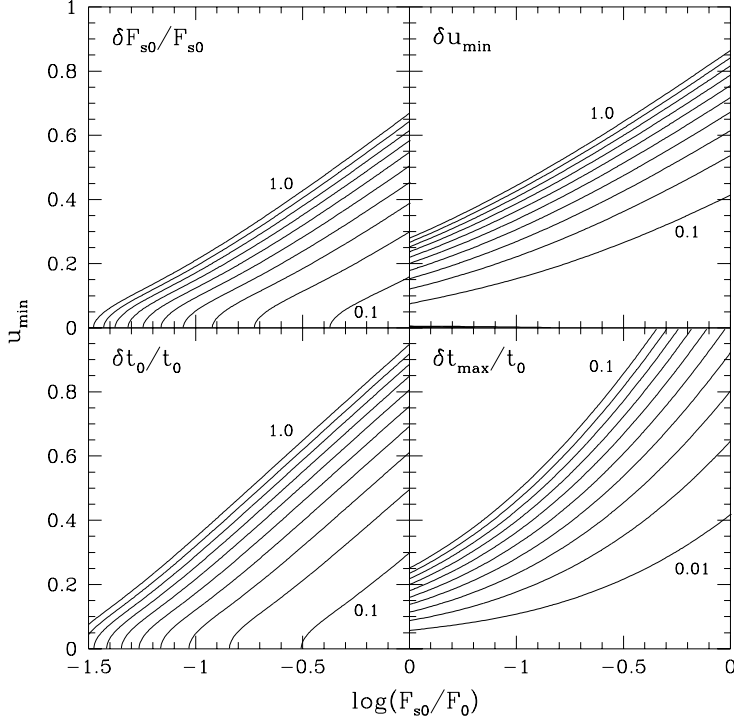


Fig. 3.— The accuracy of the best fit parameters (68% confidence) as a function of u_{min} and F_{s0}/F_0 . The lines correspond to a constant error in the best fit value determination for a given parameter. For F_{s0}/F_0 and t_0 the fractional errors are shown. The errors in t_{max} are in units of t_0 , while the errors in u_{min} are in units of Einstein radius. The lines are equally spaced in error value, between 0.1 to 1.0 for F_{s0} , u_{min} and t_0 , and from 0.01 to 0.1 for t_{max} . All parameters are best measured when the impact parameter u_{min} and the blend contribution $(F_0 - F_{s0})/F_0$ are both small, i.e. in the lower right hand corners of every panel. The photometric accuracy parameter $a \equiv \Delta_0/\sqrt{n} = 0.007$ was adopted. The plotted errors scale linearly with a provided that the number of photometric measurements n is large and the photometric error Δ_0 is small.

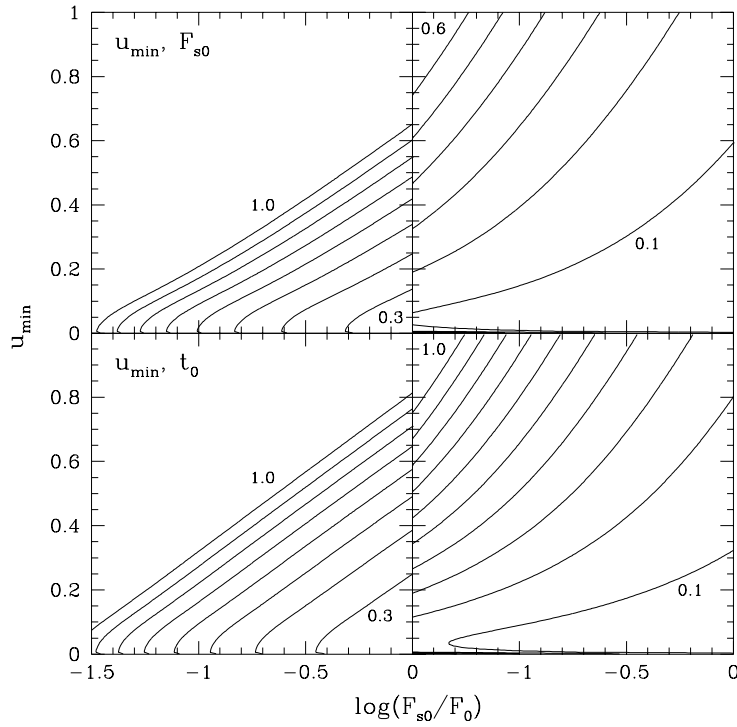


Fig. 4.— The same as Fig. 3 but for two linear combinations of $(u_{min}, F_{s0}/F_0)$ (upper panels) and (u_{min}, t_0) (lower panels), with the two combinations corresponding to the long axis of confidence ellipse (the largest errors, left panels), and the short axis of the ellipse (the smallest errors, right panels).

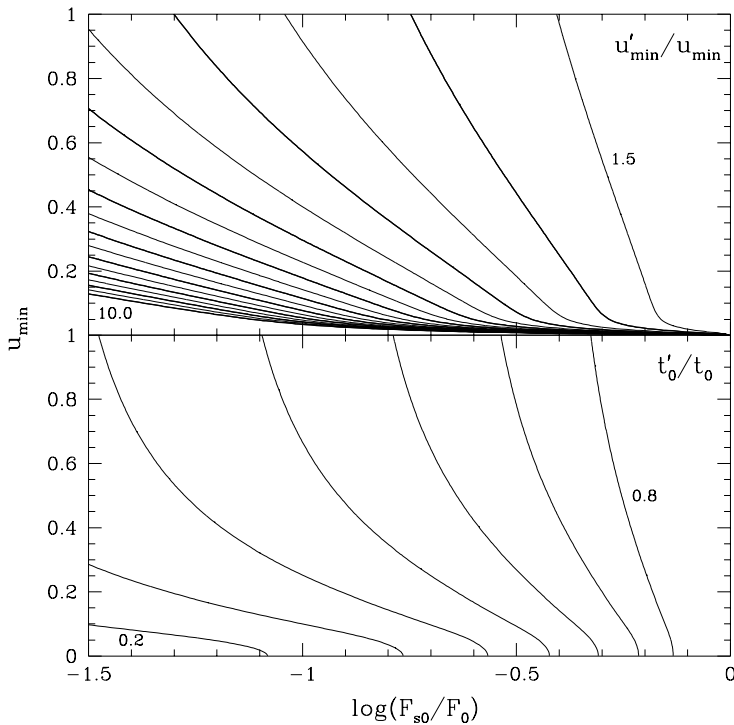


Fig. 5.— The effects of fitting a standard light curve (without a blend) to the blended microlensing events. The plots show the ratio of the best fit value of u'_{min} (upper panel) and t'_0 (lower panel) as a function of $\log(F_{s0}/F_0)$ and u_{min} . If blending is ignored then the impact parameter u_{min} is overestimated and the timescale t_0 is underestimated. The lines are labeled with the values of u'_{min}/u_{min} and t'_0/t_0 , and are equally spaced in these values.

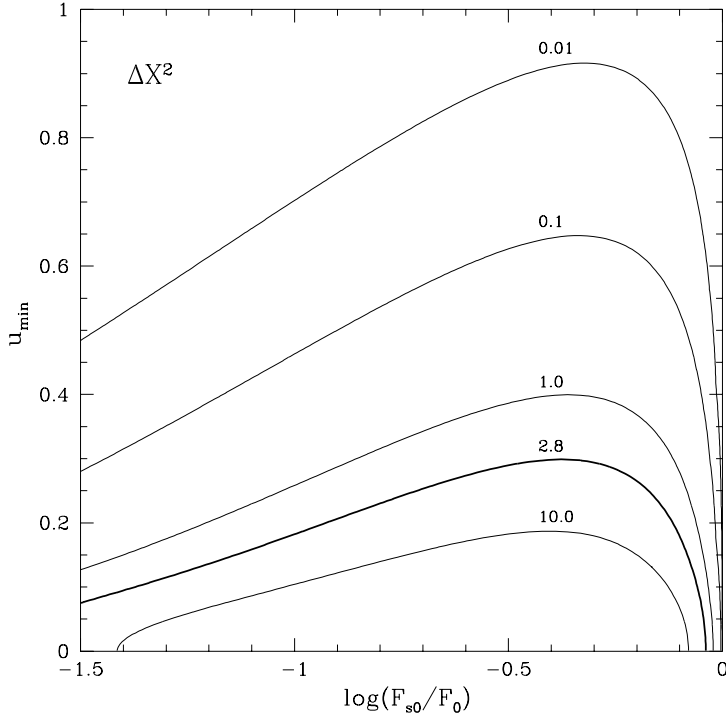


Fig. 6.— The difference ΔX^2 between the best fit model with $F_{s0} = F_0$ and the best fit model with adjustable F_{s0} is shown as a function of the impact parameter u_{\min} and the fraction of the lensed light F_{s0}/F_0 . Solid lines correspond to $\Delta X^2 = 0.01, 0.1, 1.0$, and 10.0 for the photometric accuracy parameter $a \equiv \Delta_0/\sqrt{n} = 0.007$. It is impossible to discriminate statistically between the two types of models for $\Delta X^2 < 2.8$, i.e. above the thick line (90% confidence). The two areas of strong analytical degeneracy, one for large u_{\min} and the other for small F_{s0}/F_0 , are two parts of a single very large region. When F_{s0}/F_0 approaches 1 the weak blend cannot be detected from a light curve alone, but in this case the blend is of no practical consequence.